Stabilité temporelle de l'écoulement de Poiseuille plan pulsé à grande amplitude et effet du profil de pulsation

Gaétan Andriano, Pierre Yves Passaggia, Christian Caillol, Pascal Higelin, Harambat Fabien

Temporal stability of pulsating plane Poiseuille flow at large amplitudes

G. ANDRIANO[ab], P.-Y PASSAGGIA[a], C. CAILLOL[a], P. HIGELIN[a], F. HARAMBAT[b]

a. Univ. of Orléans, INSA-CVL, PRISME, EA 4229, 45072, Orléans, France,
gaetan.andriano@stellantis.com, pierre-yves.passaggia@univ-orleans.fr,
christian.caillol@univ-orleans.fr, pascal.higelin@univ-orleans.fr
b. Advanced Research Department, STELLANTIS, 78943, Vélizy-Villacoublay, France,
fabien.harambat@stellantis.com

Résumé :

Les écoulements pulsés revêtent une importance particulière dans le contrôle des échnages de masse, quantité de mouvement et de chaleur pour des applications industrielles. La pulsation permet soit de stabiliser, soit de déstabiliser l'écoulement de Poiseuille plan suivant, d'une part, la fréquence de pulsation et, d'autre part, l'amplitude de cette dernière. Cette étude s'intéresse au rôle de la pulsation sur la stabilité de l'écoulement afin de déterminer la courbe de stabilité neutre en fonction du nombre de Reynolds, du nombre de Womersley et de l'amplitude de pulsation. Afin d'explorer une plus large gamme de paramètres, deux techniques sont combinées : l'analyse de Floquet et une méthode asymptotique WKB. Les deux approches sont complémentaires et la stabilité neutre est obtenue pour une large gamme de paramètres. Une certaine plage de Womersley, où les deux méthodes peuvent être appliquées, a été évaluée et validée. Les outils présentés dans cette étude permettent d'identifier les régimes d'écoulement et la frontière de la transition à la turbulence pour des applications automobiles en vue du contrôle du mélange dans des environnements confinés.

Abstract :

Pulsating flows are of particular importance in flow control and transition to turbulence for industrial and natural applications. Pulsation can either have a stabilising or destabilising effect and we consider the case of the plane Poiseuille plane flow in this study. In particular, we investigate the role of the pulsation frequency and amplitude on the stability of the flow in order to determine the neutral stability curve as a function of the Reynolds number, the Womersley number, and the amplitude. In order to explore a wider range of parameters, two techniques are combined: the direct matrix approach and an asymptotic WKB method. The two approaches are complementary and the neutral stability is obtained for a wide range of parameters. For a small Womersley range, both methods can be applied and this region of the control parameter is used for validation. The tools presented in this study allow for the identification of flow regimes where the transition from laminar to turbulence becomes relevant in the scope of automotive applications, for instance when considering mixing in confined environments.

Mots clefs : Pulsating parallel flow, large amplitude, Floquet's temporal stability

1 Introduction

Pulsating flows are ubiquitous in several natural flows and engineering applications but their dynamics, and in particular, their stability remains poorly understood compared to their steady counterpart. The dynamics of purely oscillating flows, on flat plates or in pipes [1], [2], [3] have received increasing attention, but rather few studies have focused on pulsating flows, comprising a steady component and an oscillation. In the human body, studies have been carried out on the behaviour of a pulsating flows in arteries [4] or through models of abdominal aortic aneurysms in S.S. Gopalakrishnan, B. Pier and A. Biesheuvel [5].

On the engineering side, heat transfer under pulsating flow conditions has been investigated in a wide variety of applications such as compact heat exchangers [6], [7] in order to enhance the heat-transfer coefficient, exhaust manifold of reciprocating engines to optimise the efficiency of internal combustion engines through waste energy recovery [8]. The results of these studies showed that optimal parameters for the pulsation (frequency and amplitude) could lead to a substantial increase of the heat transfer coefficient. In order to cover a wide range of parameters, two analyses are compared in the present work in order to identify the flow destabilisation regimes. The objective is to predict the pulsation parameters that promote fluid mixing in a confined environment. The flow regimes investigated correspond to characteristic Reynolds numbers encountered in thermal-fluid systems for automobile applications.

When considering pulsating flows, the oscillating part can be of different nature but in most cases, it is considered as sinusoidal. This pulsation will then be repeated in a cyclic way in time where a period of oscillation T will be characterised by the inverse of the pulsation frequency. In what follows, we extend the work of Pier & Schmid [9] to large-amplitude oscillations in order to establish the neutral curve for the entire control parameter set. In order to circumvent the computational time associated with the resolution of the stability problem, we propose a method based on the WKB (Wentzel-Kramers-Brillouin) approximation [10]. This method has already been adopted by Passaggia *et al.* [11] on a transient growth problems in thin-interface internal solitary waves but is only applicable for cases where the pulse frequency is very small (i.e. low Womersley numbers). The present study is organised as follows: first the mathematical tools applied to pulsating flows are presented, an introduction of the two methods of resolution are then summarised, and finally, the results collected from both methods are discussed and conclusions are drawn. This work was carried out in the scope of a Cifre thesis within the OpenLab Energetics, between STELLANTIS and the PRISME laboratory.

2 Mathematical approach

2.1 Governing equation

The main point of this study is to analyse the stability of a pulsed plane Poiseuille flow at large amplitudes using two different approaches based on very different methods: First we present the Floquet multipliers' problem where the full eigenvalue matrix problem is solved and then a WKB approach.

The velocity field $\mathbf{u}(\mathbf{x},t)$ and pressure field $p(\mathbf{x},t)$ both depend on space $\mathbf{x}$ and time t. The flow is described by the incompressible Navier-Stokes equations given by

$$\nabla \cdot \mathbf{u} = 0 \tag{2.1}$$

$$\frac{\partial \mathbf{u}}{\partial t} + (\mathbf{u} \cdot \nabla)\mathbf{u} = -\nabla p + \nu \nabla^2 \mathbf{u} \tag{2.2}$$

where ν is the kinematic viscosity of the fluid.
The problem is sought as a parallel flow between two solid boundaries where non-slip condition are implemented. We consider a cartesian reference frame where the spatial coordinate is defined as $\mathbf{x} = x\mathbf{e}_x + y\mathbf{e}_y + z\mathbf{e}_z$, where x, y and z (respectively $\mathbf{e}_x$, $\mathbf{e}_y$ and $\mathbf{e}_z$) represent the streamwise, wall-normal and spanwise coordinates, and the height of the channel is $2h$.

2.2 Base flow, disturbance and control parameters

The flow is split between a base flow and a disturbance whose amplitude is small. The solution is thus decomposed into

$$\mathbf{u}(\mathbf{x},t) = \mathbf{U}(\mathbf{x},t) + \mathbf{u}'(\mathbf{x},t) \quad \& \quad p(\mathbf{x},t) = P(\mathbf{x},t) + p'(\mathbf{x},t) \tag{2.3}$$

The Reynolds number is based on the half-height of the channel and the maximum velocity of the Poiseuille velocity profile is as $y = 0$.

Substituting the decomposition (2.3) into the incompressible Navier-Stokes equations (2.1)−(2.2) and cancelling nonlinear terms, it follows that the linearised perturbation dynamics are governed by

$$\nabla \cdot \mathbf{u}' = 0 \tag{2.4}$$

$$\frac{\partial \mathbf{u}'}{\partial t} + (\mathbf{u}' \cdot \nabla)\mathbf{U} + (\mathbf{U} \cdot \nabla)\mathbf{u}' = -\nabla p' + \frac{1}{Re}\nabla^2 \mathbf{u}' \tag{2.5}$$

where $\mathbf{U} = (U,V,W)^T$ is the base flow velocity vector and $\mathbf{u}' = (u',v',w')^T$ is the perturbation velocity vector. In the present case, the base flow is only dependent in the streamwise direction, and the base flow simplifies to $\mathbf{U} = (U(y,t),0,0)^T$.

2.3 Pulsating Poiseuille flow

This section follows the work in [9] and some definitions are introduced because of the pulsating nature of the flow. In the present work, we consider a single frequency Ω. The time-dependent baseflow remains only dependent on the streamwise direction and solely varies along the wall-normal coordinate y. The solution is therefore expanded as

$$U(y,t)\mathbf{e}_\mathbf{x} = \hat{U}^{(0)}(y) + \sum_{n\neq 0} \hat{U}^{(n)}(y)\exp(\mathrm{i}n\Omega t), \tag{2.6}$$

and it is affiliated to a spatially uniform and temporally periodic streamwise pressure gradient of the form $G(t)\mathbf{e}_\mathbf{x}$, where

$$G(t) = \hat{G}^{(0)} + \sum_{n\neq 0} \hat{G}^{(n)}\exp(\mathrm{i}n\Omega t). \tag{2.7}$$

Whence, the temporally periodic base flow rate writes

$$Q(t) = \hat{Q}^{(0)} + \sum_{n\neq 0} \hat{Q}^{(n)} \exp(\mathrm{i}n\Omega t). \tag{2.8}$$

When $n < 0$ and in order to ensure that all quantities are real, the associated complex conjugate has to be included and there exists a relationship between the flow rate $\hat{Q}^{(n)}$ and the velocity component $\hat{U}^{(n)}$ such that

$$\hat{U}^{(n)}(y) = \frac{\hat{Q}^{(n)}}{2h} \mathscr{W}(\xi, \mathscr{N}) \tag{2.9}$$

where $\xi = y/h$, $\mathscr{N} = \sqrt{n}Wo$, and the Womersley number Wo is defined as $Wo = h/\delta = h\sqrt{\Omega/\nu}$, where δ refers to the thickness of the oscillating boundary layer near the wall (i.e. the Stokes boundary layer).

The different components of the base flow $\mathscr{W}$ refer to the profile of the different unsteady velocity components and are given by

$$\mathscr{W}(\xi, \mathscr{N}) = \begin{cases} \left(\frac{\cosh(\sqrt{\mathrm{i}}\xi\mathscr{N})}{\cosh(\sqrt{\mathrm{i}}\mathscr{N})} - 1\right) \Big/ \left(\frac{\tanh(\sqrt{\mathrm{i}}\mathscr{N})}{\sqrt{\mathrm{i}}\mathscr{N}} - 1\right) & \text{if} \quad \mathscr{N} \neq 0 \\ \frac{3}{2}(1-\xi^2) & \text{if} \quad \mathscr{N} = 0 \end{cases} \tag{2.10}$$

where $\sqrt{\mathrm{i}} \equiv (\mathrm{i}+1)/\sqrt{2}$.
Furthermore, the pressure and the flow rate components are also related as

$$\frac{\hat{Q}^{(n)}}{\hat{G}^{(n)}} = \begin{cases} 2\frac{h^3}{\nu} \frac{\mathrm{i}}{n\mathrm{Wo}^2} \left(\frac{\tanh(\sqrt{\mathrm{i}}\mathscr{N})}{\sqrt{\mathrm{i}}\mathscr{N}} - 1\right) & \text{if} \quad n \neq 0 \\ \frac{2}{3}\frac{h^3}{\nu} & \text{if} \quad n = 0 \end{cases} \tag{2.11}$$

To simplify the calculation, a single oscillating component has been investigated (*i.e.* $n = -1$, $n = 0$ or $n = 1$), similar to [9].

In order to remain consistent with the non dimensionalisation, the pulse frequency is defined as $\Omega = Wo^2/Re$, and the period of a pulsation is $T = 2\pi Re/Wo^2$. Additionally, as specified in [9], we define a pulsation amplitude relative to the mass-flow rate, isolating the real part of (2.8) which writes

$$\tilde{Q} = 2Q^{(1)}/Q^{(0)} \quad \text{providing} \quad Q(t) = Q^{(0)}(1 + \tilde{Q}\cos(\Omega t)) \tag{2.12}$$

The evolution of the base flow over full period is shown in figure 1. A pulsatile flow is a sum between a stationary velocity profile (mode 0) and an oscillating velocity profile (mode 1). Mode 0 is the Poiseuille profile. The first mode of oscillation is defined according to equation (2.11). Note the presence, of the two conditions for linear instability [12], namely: the Rayleigh inflection point criterion and the Fjørtoft criterion are met. Indeed, at large amplitudes, there is a strong presence of a backflow, and up to four inflection points may appear during the pulsation period (as shown in figure 1).

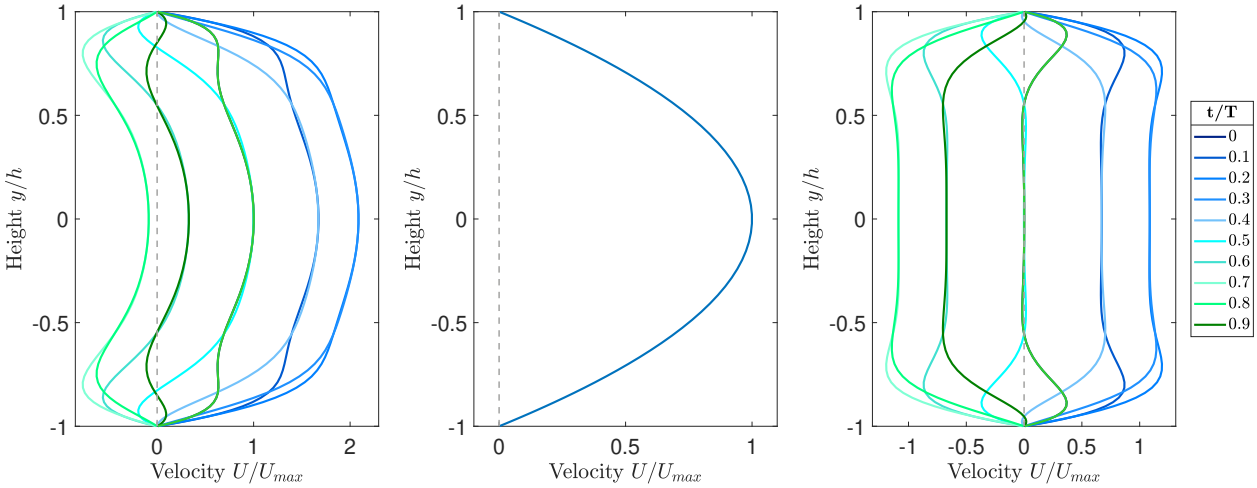

Figure 1: Profile of the basic velocity field at 10 different times. On the left, combination of stationary and oscillating profile. In the middle, Poiseuille profile in stationary regime (mode 0). On the right, pulsation component (mode 1). In the case presented, $Re = 7500$, $Wo = 10$, $\tilde{Q} = 1.6$, $\alpha = 1$, $\beta = 0$.

3 Stability analysis

3.1 Matrix approach to the Floquet's stability of time-dependent base flows

Now that the symmetric base flow is obtained perturbations are expanded into harmonic plane waves in the parallel directions of the flow and also comprise the pulse frequency Ω. Each of these disturbances are related to the harmonic disturbance frequencies m, which are written as Fourier series such that

$$\mathbf{u}'(\mathbf{x},t) = \left[\sum_m \hat{\mathbf{u}}^{(m)}(y)\exp(\mathrm{i}m\Omega t)\right]\exp[\mathrm{i}(\alpha x+\beta y-\omega t)], \tag{3.1}$$

$$p(\mathbf{x},t) = \left[\sum_m \hat{p}^{(m)}(y)\exp(\mathrm{i}m\Omega t)\right]\exp[\mathrm{i}(\alpha x+\beta y-\omega t)], \tag{3.2}$$

where α, $\beta \in \mathbb{R}$ are the streamwise and spanwise wavenumbers, and $\omega \in \mathbb{C}$ is a complex frequency.

Introducing the decomposition (3.1)−(3.2) into the linearized Navier-Stokes equations (2.4)−(2.5), the temporal stability can be obtained by computing the eigenvalue problem [9]

$$\begin{cases} 0 = \alpha\hat{u}^{(m)} - \mathrm{i}\dfrac{\partial\hat{v}^{(m)}}{\partial y} + \beta\hat{w}^{(m)}, & (3.3)\\ \omega\hat{u}^{(m)} = n\Omega\hat{u}^{(m)} + \alpha\displaystyle\sum_q U^{(q)}\hat{u}^{(m-q)} + \mathrm{i}Re^{-1}\nabla^2\hat{u}^{(m)} - \mathrm{i}\sum_q \frac{\partial\hat{U}^{(m)}}{\partial y}\hat{v}^{(m-q)} + \alpha\hat{p}^{(m)}, & (3.4)\\ \omega\hat{v}^{(m)} = n\Omega\hat{v}^{(m)} + \alpha\displaystyle\sum_q U^{(q)}\hat{v}^{(m-q)} + \mathrm{i}Re^{-1}\nabla^2\hat{v}^{(m)} - \mathrm{i}\frac{\partial\hat{p}^{(m)}}{\partial y}, & (3.5)\\ \omega\hat{w}^{(m)} = n\Omega\hat{w}^{(m)} + \alpha\displaystyle\sum_q U^{(q)}\hat{w}^{(m-q)} + \mathrm{i}Re^{-1}\nabla^2\hat{w}^{(m)} + \beta\hat{p}^{(m)}. & (3.6) \end{cases}$$

One can substitute the pressure term and simplify the above system using the wall-normal velocity and the vorticity defined as $\eta = \partial_z u - \partial_x w$. The system therefore simplifies to

$$\begin{cases} \omega \nabla^2 \hat{v}^{(m)} = n\Omega \hat{v}^{(m)} + \mathrm{i}Re^{-1}\nabla^4 \hat{v}^{(m)} + \alpha \sum_q U^{(q)} \nabla^2 \hat{v}^{(m-q)} - \alpha \sum_k \hat{U}''^{(q)} \hat{v}^{(m-q)}, & (3.7) \\ \omega \hat{\eta}^{(m)} = n\Omega \hat{\eta}^{(m)} + \mathrm{i}Re^{-1}\nabla^2 \hat{\eta}^{(m)} + \alpha \sum_k \hat{U}^{(q)} \hat{\eta}^{(m-q)} - \mathrm{i}\beta \sum_k \hat{U}'^{(q)} \hat{v}^{(m-q)}, & (3.8) \end{cases}$$

where $\nabla^2 = \partial^2/\partial y^2 - k^2$ and $k^2 = \alpha^2 + \beta^2$.

The system (3.8) is the Floquet form of the Orr-Sommerfeld and Squire equation system. We can clearly see that there exists interactions between the base flow and the perturbation through the infinite sums on the right-hand side which may eventually be truncated for the resolution. The system (3.7)−(3.8) results in a matrix system where the modes $m = -1$, $m = 0$, $m = 1$ will constitute a tridiagonal set of sub-matrices. The sub-matrices are of dimension $(N \times N)$, where N is the number of Chebyshev polynomials. Consequently, the total size of the stability matrix to be solved is of order $(N \times N_f) \times (N \times N_f)$ where N_f represents the number of Fourier modes that will have to be retained in order to ensure convergence of the spectrum associated with ω.

The solution is a complex set of eigenvalues of ω where the imaginary part represents the growth rate and the real part the angular frequency. Similarly to the classical stability analysis, the goal is to identify the eigenvalues that have the largest growth rate. If $\omega_i > 0$, the flow is convectively unstable and otherwise stable.

3.2 WKB method

When the angular frequency of the baseflow Ω is small when compared to the angular frequency of the disturbance ω_r, the problem can be further simplified and a WKB approach (Wentzel-Kramers-Brillouin) method can be sought. This method assumes that the harmonics m between the pulsating baseflow and the perturbations become small and that only the instantaneous base velocity profiles play a role.

Unlike the matrix approach to Floquet's analysis where time is sought as a Fourier series, the WKB method gets rid of this costly decomposition by assuming that the baseflow is time dependent but that the harmonics m can be neglected. For this, we start again from the formulations established in §2.3. The pulsating streamwise velocity component relative to the base frequency Ω can be expressed as the sum of the Poiseuille solution (mode 0) and the oscillatory component (mode 1). Taking into account the evolution in time, and keeping only the real part, this amounts to writing

$$\hat{U}(y,t) = \hat{U}^{(0)}(y) + \Re\left\{\hat{U}^{(1)}(y)e^{\mathrm{i}\Omega t}\right\} + \Re\left\{\hat{U}^{(-1)}(y)e^{-\mathrm{i}\Omega t}\right\} \quad (3.9)$$

where the associated steady pressure gradient is $G^{(0)} \equiv 2/\mathrm{Re}$ and $G^{(1)}$ will depend on the adopted pulse amplitude $\tilde{Q}$.

Next, we compute the eigenvalues of the Orr-Sommerfeld and Squire equations at each instant of the

pulse, as described in equations (3.10)−(3.12).

$$\omega \begin{pmatrix} \nabla^2 & 0 \\ 0 & 1 \end{pmatrix} \begin{pmatrix} \hat{v} \\ \hat{\eta} \end{pmatrix} + \begin{pmatrix} M_{OS} & 0 \\ \beta \hat{U}'(y,t) & M_{SQ} \end{pmatrix} \begin{pmatrix} \hat{v} \\ \hat{\eta} \end{pmatrix} = 0 \tag{3.10}$$

where

$$M_{OS} = \alpha \hat{U}(y,t)\left(\mathscr{D}^2 - k^2\right) - \alpha \hat{U}''(y,t) + \mathrm{i}Re^{-1}\nabla^4 \tag{3.11}$$

$$M_{SQ} = \alpha \hat{U}(y,t) + \mathrm{i}Re^{-1}\nabla^2 \tag{3.12}$$

The aim is to track the eigenvalue in the complex plane to compute the growth rate during a single pulse period. These growth rates are, in fine, integrated over the whole pulsation period and are expected to match the eigenvalues obtained from the full matrix form (3.8). The solution, which comes at a little computational cost writes

$$\omega_{i\ global} \equiv \int_0^T \omega_{i\ local}(t,k)\mathrm{d}t. \tag{3.13}$$

Using this formulation, it is possible now to investigate the stability characteristics of pulsating flows for a wide range of parameters such as amplitude $\tilde{Q}$, Reynolds numbers Re, and Womersley numbers Wo.

4 Results

4.1 Validation of Floquet analysis

The first part aims at validating the present approach. For this purpose, we compare our results with the figure 7 in [9] as a reference, where the maximum growth rates for different pulse cases are presented in the range $5 \leqslant Wo \leqslant 25$; $0 \leqslant \tilde{Q} \leqslant 0.6$. The same range of data was tested for $N_f = 40$ Fourier modes and $N = 36$ Chebyshev polynomials. Figure 2, provides an overview of the growth rates computed from equation (3.8). These curves are almost identical to the ones obtained in [9], and therefore validate our implementation. We note that some growth rates have diverged from a certain amplitude. As shown in [9], it is the number of Fourier modes that is insufficient in order to converge all the branches of the spectrum, and hence, the maximum growth rate.

From this reference code, several pulsation regimes were explored, in particular low Reynolds number regimes, which are theoretically stable without pulsation but which are investigated here in order investigate the destabilising nature of the pulsatile component to the flow. The idea is to explore how growth rates behave for large values of the pulsation amplitude $\tilde{Q}$ and small values of Re.

Figure 3 shows the linear dynamics of the flow at $Re = 4000$, for a range of pulsation $0 \leqslant \tilde{Q} \leqslant 1.8$ and for $Wo = [5;7;9;11;13;15]$. When $\tilde{Q} = 0$, we fall back on the classical Orr-Sommerfeld equation which predicts that the flow is stable for a Reynolds value lower than 5772.2, the critical Reynolds value when $\alpha = 1$. As before, high Womersley numbers (here about more than 10) have a stabilising effect the flow when the pulsation amplitude is increased. For $Wo = 5$ and $Wo = 7$, the growth rate increases slowly with the amplitude until it reaches a maximum. Then, it decreases and reaches a somewhat constant growth rate at $\tilde{Q} = 1.8$. Increasing the pulse amplitude does not necessarily means that the growth rate will follow the same trend and increases. For these same Womersley numbers, it is possible to

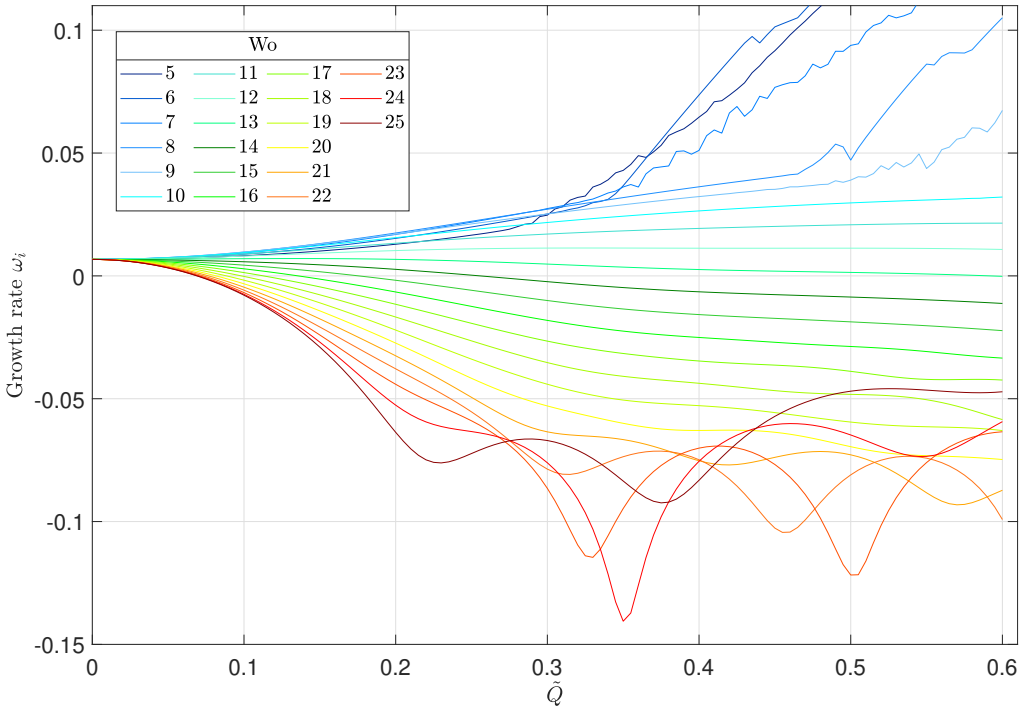

Figure 2: Validation of maximum growth rate as a function of Re, Wo and $\tilde{Q}$, with $N = 40$ and $N_f = 36$.

destabilise the flow for certain pulsation regimes, whereas it was theoretically stable in the stationary regime. This supports the results in [9] who showed that the critical Reynolds number is influenced by the amplitude of the pulsation. Indeed, for low Womersley numbers, the critical Reynolds which defines the boundary between stable and transient flow is lower than the critical Reynolds number in the pulsation-free regime. At high Womersley, the critical Reynolds number is higher and it becomes more difficult to destabilise the flow. Finally, at $Wo = 7$, when the amplitude becomes higher than $\tilde{Q} \approx 1.18$, the pulsation will have a stabilising effect whereas an unsteady state had been established for $0.38 \leqslant \tilde{Q} \leqslant 1.18$.

The matrix approach to the Floquet analysis is very accurate and relatively simple to implement. On the other hand, its weak point is the computational power necessary to resolve the spectrum which increases drastically with the number of Fourier modes when the Womersley number decreases and/or when the pulsation amplitude increase. Whence, the WKB was considered as an alternative to explore these slow-pulsating regimes.

4.2 Matrix approach vs. WKB method

Compared to the matrix approach, where the eigenvalue problem is solved taking into account m Fourier modes, the WKB approximation is a time integration method, where the maximum growth rates are extracted at different times of the pulsation. In order to obtain accurate approximations to the eigenvalue spectrum, the time step must be small. Figure 4 illustrates the method where the shaded part represents the integration in time which will give our global growth rate for a pulsation and which we will compare with the value obtained with the Floquet analysis. However, as the theory of the WKB method has been posed, only cases of pulsations with a very long time, i.e. low frequencies, will be studied.

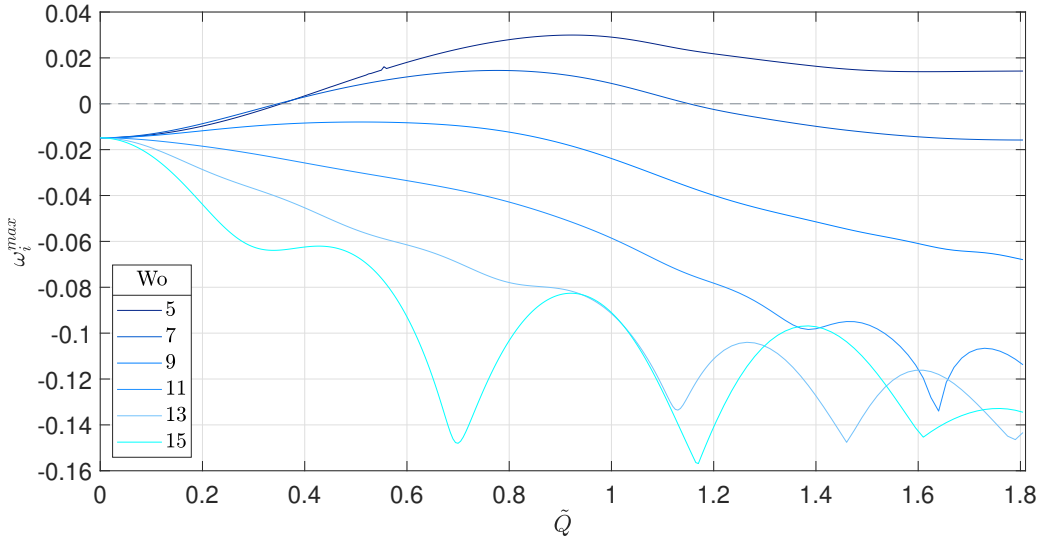

Figure 3: Linear dynamics at $Re = 4000$ and $\alpha = 1$ for $0 \leqslant \tilde{Q} \leqslant 1.8$ and $5 \leqslant Wo \leqslant 15$, with $N = 32$ and $N_f = 20$.

As proposed in J.S. Kern *et. al* [13], individual eigenvalues are tracked at different time instants. Figure 4 shows the evolution of the leading eigenvalue at $Re = 7500$, $\tilde{Q} = 0.3$, and $Wo = 5$. In figure 5a, the spectrum of the case studied at $Re = 7500$, $Wo = 5$, $\tilde{Q} = 0.3$ where the evolution of the eigenvalue is tracked in the upper left corner, and shown in red. The temporal evolution of this eigenvalue leads to the shape shown in blue in figure 5b. Therefore, the global growth rate amounts to integrating the area enclosed in this surface.

Once an eigenvalue of interest is identified, different pulsation amplitudes, Reynolds numbers, and Womersley numbers were investigated, and this, for the same parameters than computed than for the matrix approach . The goal is to validate this approach.

In figure 6, the growth rate ω_i is shown as a function of the amplitude $\tilde{Q}$, which varies from 0 to 0.1, and for different Womersley numbers. Six Womersley cases were computed, from $Wo = 5$ to $Wo = 10$. The figure has been voluntarily split into two, with on one side, the odd Womersley numbers, and on the other, the even Womersley numbers, for the ease of visualisation. The WKB method provides a good approximation of the growth rate for all the cases studied. Nevertheless, we observe a slight departure when the Womersley number increases. This is to be expected as the baseflow frequency increases and no longer separates from the perturbations frequency. On the other hand, since the growth rates are computed at fixed time instants, some physical interactions are not taken into account such as the transport phenomena of the base field which will interact with the perturbations. However, the WKB method remains a valuable tool to investigate low Womersley numbers, and this, for all Reynolds numbers.

The analysis was undertaken to larger amplitudes but the WKB method leads to another limitation. As shown in figure 7 (red points) and figure 5b (boxed area), increasing $\tilde{Q}$ leads to a discontinuity in the eigenvalue path. This discontinuity has not been yet documented and we speculate that this behaviour may be associated with a new phenomena. This prevents the eigenvalue from returning to its initial position, at the end of the pulsation. This singularity will become more pronounced as the pulsation amplitude $\tilde{Q}$ increases. The appearance and understanding of this phenomenon is an integral part of the

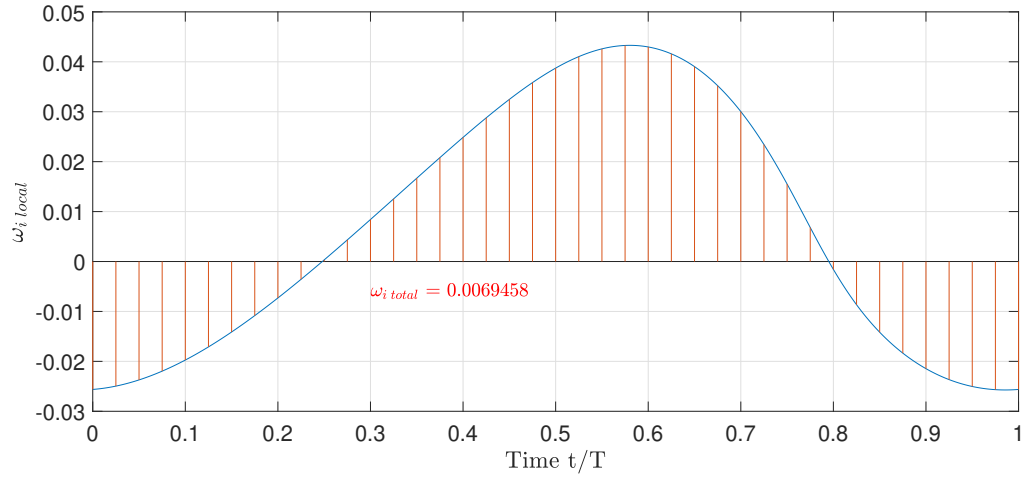

Figure 4: Evolution of the maximum growth rate as a function of time. The blue line represents the growth rates extracted at each instant and the hatched area is our maximum growth rate over a full pulsating period. $Re = 7500$, $\tilde{Q} = 0.3$, and $Wo = 5$

new research work currently being investigated.

An important feature of the WKB approach is its simulation time compared to the Floquet analysis. Tables 1 and 2 report the simulation times of the two methods. Note that the calculations were performed on the same computer. The number of Chebyshev points was fixed at $N = 63$ and the calculation for the matrix approach was performed on a graphical processor unit, unlike the WKB method. It can be seen that in all cases, the WKB method is substantially faster. The number of temporal points N_t chosen is a compromise between computation time and accuracy of the computed growth rate but it could be lowered in some cases. At $Wo = 7$ and $Wo = 9$, no value could be calculated due to the appearance of the discontinuity in the spectra. The time of the calculations for the Floquet method is strongly dependent on the number of Fourier modes. However, it is essential to consider a sufficient number of Fourier modes N_f in order to converge the growth rates.

$Re = 3000$	$Wo = 5$	$Wo = 7$	$Wo = 9$
$\tilde{Q} = 0.1$	10.7	2.11	2.15
$\tilde{Q} = 0.3$	37.64	10.46	10.41
$\tilde{Q} = 0.6$	93.51	36.68	36.24
$N_f =$	$20 \rightarrow 40$	$10 \rightarrow 30$	$10 \rightarrow 30$

Table 1: Computation time Floquet analysis

$Re = 3000$	$Wo = 5$	$Wo = 7$	$Wo = 9$
$\tilde{Q} = 0.1$	4.63	4.65	4.63
$\tilde{Q} = 0.3$	4.64	4.64	4.62
$\tilde{Q} = 0.6$	4.62	–	–
$N_t =$	600	600	600

Table 2: Computation time WKB method

4.3 Neutral curves

Next, we report the neutral stability curves according to different pulse cases considered in this analyse. Neutral curves allow us to discern the boundary between a stable regime and a unstable (transitional) regime. In the present case, we aim at examining the influence of the pulsation on the perturbations dynamics and thus, identify the cases that provide the largest growth rates.

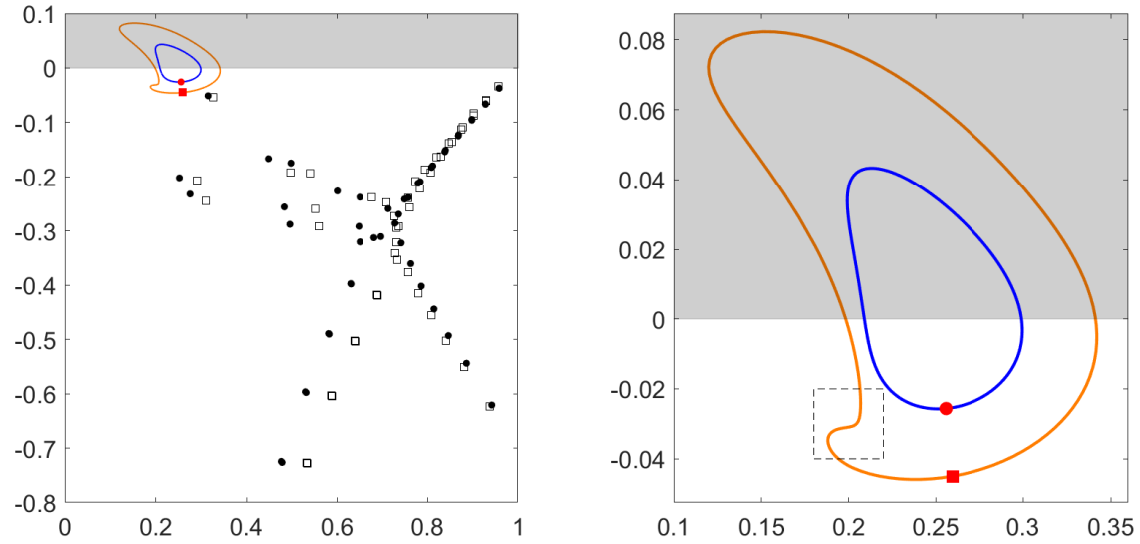

(a) Spectrum of a pulsation and identification of the maximum growth rate.

(b) Temporal evolution of our maximum growth rate. $\tilde{Q} = 0.3$ (blue), $\tilde{Q} = 0.555$ (orange)

Figure 5: Eigenvalue tracking in the complex plane. The shaded part symbolises the area where $\omega_i > 0$, *i.e.*, when our flow is unstable. $Re = 7500$, $Wo = 5$, and $\tilde{Q} = 0.3$ ($*$), $\tilde{Q} = 0.555$ ($\square$)

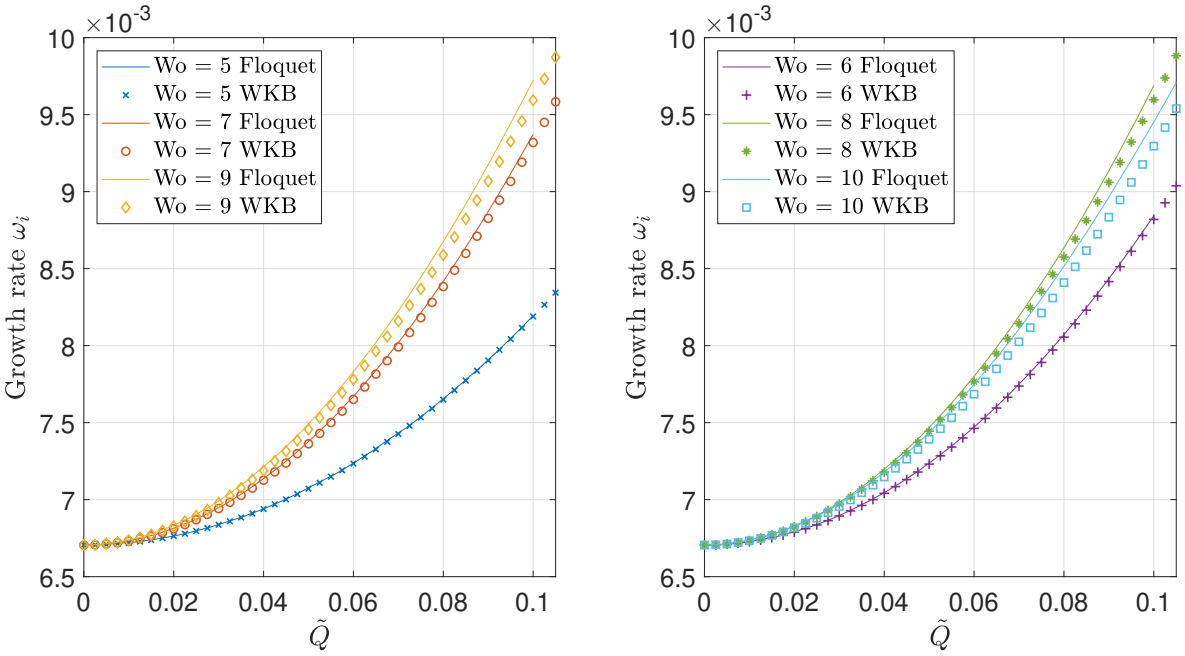

Figure 6: Comparison of the linear dynamics of the Floquet analysis and the WKB approximation for $0 \leqslant \tilde{Q} \leqslant 0.1$ and $5 \leqslant Wo \leqslant 10$, at $Re = 7500$. On the left, odd Womersley. On the right, even Womersley.

Three neutral curves are shown in figure 8 for three different Reynolds numbers ($Re = [4000; 5000; 6000]$). The pulsation amplitude $\tilde{Q}$ varies between 0 and 1.4 and Womersley numbers Wo in the range $[1, 15]$. For $1 \leqslant Wo \leqslant 5$, the WKB approach was used and for $5 \leqslant Wo \leqslant 15$ the matrix approach. First, when increasing the Reynolds number, the growth rate, whatever the generated pulse increases. The fluid being the same from one case to another, the viscous effects remain unchanged.

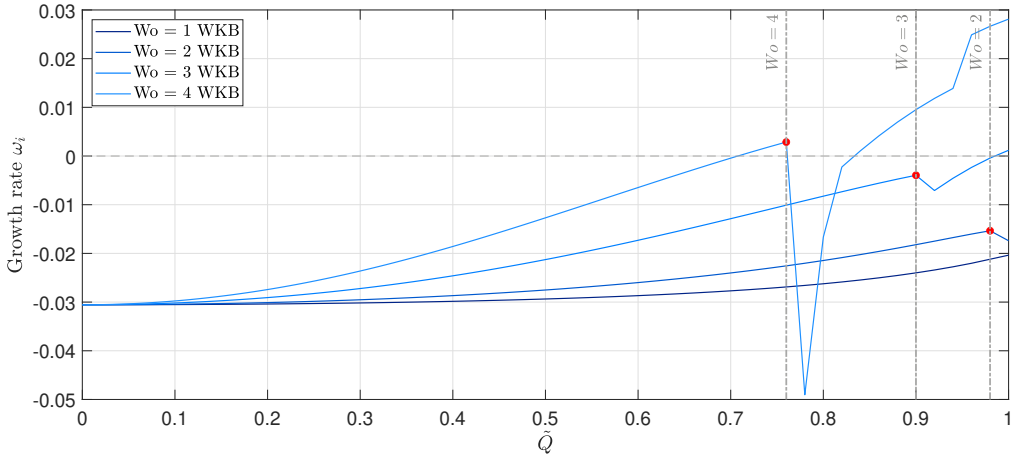

Figure 7: Linear dynamics by WKB method for $0 \leqslant \tilde{Q} \leqslant 1$ and $1 \leqslant Wo \leqslant 4$, at $Re = 3000$. We observe a divergence at $Wo = 2$,$Wo = 3$,$Wo = 4$ when $\tilde{Q} = 0.98$, $\tilde{Q} = 0.9$, $\tilde{Q} = 0.76$ respectively.

When increasing inertial effects, the flow tends to naturally destabilise since viscous effects decrease. Again, it is possible to observe the transition of the critical Reynolds because at $Re = 6000$, when $\tilde{Q} = 0$, where the flow becomes unstable. To make the link with the work in [9], the largest growth rates are observed for low Womersley numbers, on the three studied regimes. Simultaneously, figure 3 shows that the growth rate does not evolve linearly with the amplitude $\tilde{Q}$. Depending on the Womersley number, the high-amplitude pulsation can have a stabilising effect on the flow. For example, at $Re = 5000$ and $Wo \approx 9$, the flow is unstable at $\tilde{Q} \approx 0.6$ whereas it is stable when $\tilde{Q} \approx 1.2$. We can see that for the three Reynolds number studied, the instabilities are maximum for $0.8 \leqslant \tilde{Q} \leqslant 1$ and $5 \leqslant Wo \leqslant 7$. Finally, note that the white part of the plot is either too intensive to compute using the matrix approach, or fails when attempting to use the WKB method. This is directly related to figure 7 where the appearance of the singularity in the complex plane prevents the eigenvalue from converging correctly, as shown in figure 5b with a limiting amplitude at $\tilde{Q} = 0.555$.

5 Conclusion

The research conducted in this paper aims at understanding the influence of a pulsating flow in the case of a plane Poiseuille flow. Results are compared between a stationary flow and different amplitudes as well as frequencies of oscillations. This work allows for predicting the perturbation dynamics, depending on the pulsation regime using two very distinct but complementary methods: the direct matrix approach and the WKB method.

In [9], the linear and nonlinear dynamics of a pulsating flow was similarly investigated in a planar channel with a DNS method and by Floquet analysis. Here, Floquet analysis was pursued at larger amplitudes. However increasing the pulsation amplitude does not necessarily mean that the flow will be more unstable.

The present approach allows for extending the existing results from the literature where we are now able to compute a larger range of Womersley numbers and amplitudes compared to [9]. For most Reynolds numbers, the pulsation amplitude has a either a stabilising effect rather than a destabilising

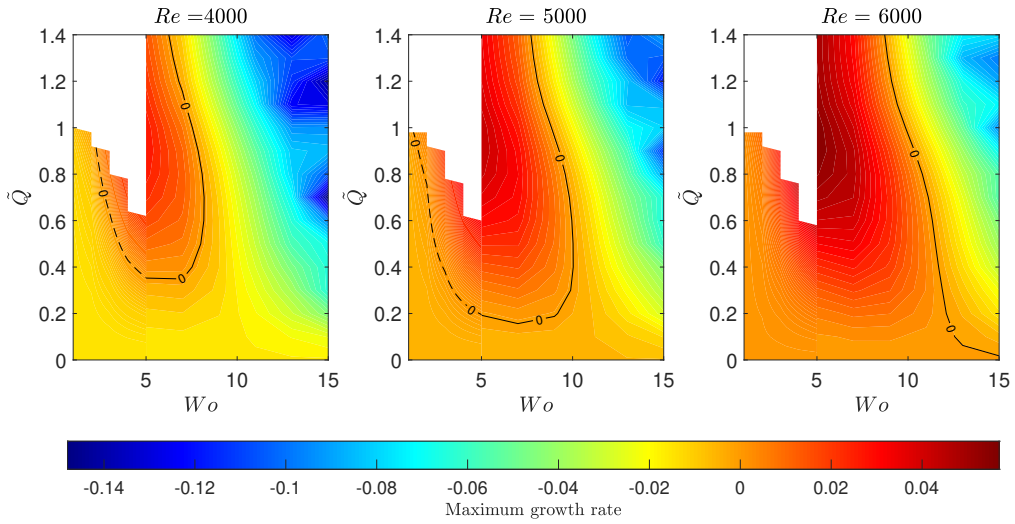

Figure 8: Neutral curve by combining the Floquet method and WKB appoximation for $\alpha = 1$, $\beta = 0$, $4000 \leqslant Re \leqslant 6000$, $0 \leqslant \tilde{Q} \leqslant 1.4$ and $1 \leqslant Wo \leqslant 15$. In the range $1 \leqslant Wo \leqslant 5$, the WKB method is used (dashed line). The white area represents the part where the calculation has diverged. In the range $5 \leqslant Wo \leqslant 15$, it is the analysis of Floquet which is presented (filled line).

one. Complementary, the WKB approach was found to be more appropriate for smaller Womersley regimes, where the pulsation period is long and therefore difficult to compute using the matrix approach. Compared to the first method which is based on a time independent matrix system composed of m Fourier modes, the WKB method solves a simpler eigenvalue problem which is only computed for different times instants during the pulsation period. This procedure is not as efficient as Floquet's analysis because as it does not take into account all the physics of our flow, but it still provides a good approximations for small Womersley numbers. When the amplitude increases beyond a certain threshold, we observe the appearance of a discontinuity in the spectrum computed using the WKB method that prevents from determining the complete stability map. This change of behaviour in the spectrum is currently under investigation in our group.

References

[1] T. Sarpkaya, Coherent structures in oscillatory boundary layers, Journal of Fluid Mechanics, 253 (1993) 105–140.

[2] G. Vittori, R. Verzicco, Direct simulation of transition in an oscillatory boundary layer, Journal of Fluid Mechanics, 371 (1998) 207–232.

[3] C. Thomas, C. Davies, A. P. Bassom, P. J. Blennerhassett, Evolution of disturbance wavepackets in an oscillatory Stokes layer, Journal of Fluid Mechanics, 752 (2014) 543–571.

[4] D.N. Ku, Blood flow in arteries, Annual review of fluid mechanics, 29 (1997) 399–434.

[5] S.S. Gopalakrishnan, B. Pier, A. Biesheuvel, Dynamics of pulsatile flow through model abdominal aortic aneurysms, Journal of Fluid Mechanics, 758 (2014) 150–179.

[6] C. Wantha, Effect and heat transfer correlations of finned tube heat exchanger under unsteady pulsating flows, International Journal of Heat and Mass Transfer, 99 (2016) 141–148.

[7] H. Khosravi-Bizhaem, A. Abbassi, A. Zivari-Ravan, Heat transfer enhancement and pressure drop by pulsating flow through helically coiled tube: An experimental study, Applied Thermal Engineering, 160 (2019) 114012.

[8] M. Simonetti, C. Caillol, P. Higelin, C. Dumand, E. Revol, Experimental investigation and 1D analytical approach on convective heat transfers in engine exhaust-type turbulent pulsating flows, Applied Thermal Engineering, 165 (2020) 114548.

[9] B. Pier, P.J. Schmid, Linear and nonlinear dynamics of pulsatile channel flow, Journal of Fluid Mechanics, 815 (2017) 435–480.

[10] C.M. Bender, S.A. Orszag, Advanced mathematical methods for scientists and engineers I: Asymptotic methods and perturbation theory, Springer Science & Business Media. (1999) 484–534.

[11] P-Y. Passaggia, K.R. Helfrich, B.L. White, Optimal transient growth in thin-interface internal solitary waves, Journal of Fluid Mechanics, 840 (2018) 342–378.

[12] P.J. Schmid, D.S. Henningson, Stability and Transition in Shear Flows, Applied mathematical sciences, vol. 142. Springer. (2001).

[13] J.S. Kern, M. Beneitez, A. Hanifi, D.S. Henningson, Transient linear stability of pulsating Poiseuille flow using optimally time-dependent modes, Journal of Fluid Mechanics, 927 (2021) 55–72.